The American Journal of Pathology, Vol. 173, No. 5, November 2008

DOI: 10.2353/ajpath.2008.071039

Molecular Pathogenesis of Genetic and Inherited Diseases

Sall1, Sall2, and Sall4 Are Required for Neural Tube Closure in Mice

Johann Böhm,* Anja Buck,† Wiktor Borozdin,*‡ Ashraf U. Mannan,† Uta Matysiak-Scholze,* Ibrahim Adham,† Walter Schulz-Schaeffer,§ Thomas Floss,¶ Wolfgang Wurst,¶ Jürgen Kohlhase,‡ and Francisco Barrionuevo*

From the Institut für Humangenetik und Anthropologie, Universität Freiburg, Freiburg; the Institut für Humangenetik,† Universität Göttingen, Göttingen; the Praxis für Humangenetik,‡ Freiburg; the Abteilung Neuropathologie,§ Universitätsklinikum Göttingen, Göttingen; and the GSF National Research Center for Environment and Health,¶ Institute of Developmental Genetics, Neuherberg, Germany*

Four homologs to the *Drosophila* homeotic gene *spalt* (*sal*) exist in both humans and mice (*SALL1* to *SALL4*/*Sall1* to *Sall4*, respectively). Mutations in both *SALL1* and *SALL4* result in the autosomal-dominant developmental disorders Townes-Brocks and Okihiro syndrome, respectively. In contrast, no human diseases have been associated with *SALL2* to date, and *Sall2*-deficient mice have shown no apparent abnormal phenotype. We generated mice deficient in *Sall2* and, contrary to previous reports, 11% of our *Sall2*-deficient mice showed background-specific neural tube defects, suggesting that *Sall2* has a role in neurogenesis. To investigate whether *Sall4* may compensate for the absence of *Sall2*, we generated compound *Sall2* knockout/*Sall4* genetrap mutant mice. In these mutants, the incidence of neural tube defects was significantly increased. Furthermore, we found a similar phenotype in compound *Sall1/4* mutant mice, and *in vitro* studies showed that SALL1, SALL2, and SALL4 all co-localized in the nucleus. We therefore suggest a fundamental and redundant function of the Sall proteins in murine neurulation, with the heterozygous loss of a particular SALL protein also possibly compensated in humans during development. *(Am J Pathol 2008, 173:1455–1463; DOI: 10.2353/ajpath.2008.071039)*

The homeotic *spalt* (*sal*) gene of *Drosophila melanogaster* determines the identity of the anterior head and the posterior tail regions in early development.[1,2] At later stages, *sal* is involved in the development of the wing disk, trachea, and sensory organs.[3–6] Humans and mice have four functional *sal*-related genes *SALL1* to *SALL4* (*Sall1* to *Sall4* in mice). The human *SALL* genes encode transcription factors presenting a characteristic structure of evenly distributed zinc finger domains. Mutations in *SALL1* result in Townes-Brocks syndrome (TBS, OMIM 107480), a rare autosomal-dominant malformation syndrome that is characterized by dysplastic ears, preaxial polydactyly and/or triphalangeal thumbs, imperforate anus, renal malformations, and heart anomalies.[7–9] Mutations in *SALL2* are not associated with any disease, however, it has been suggested that SALL2 may act as a tumor suppressor.[10,11] Deletion of *SALL3* has been implicated in the phenotype of the 18q-deletion syndrome.[12] Mutations in *SALL4* cause autosomal-dominant Okihiro/Duane-Radial Ray syndrome (DRRS, OMIM 607323), combining radial ray defects and Duane anomaly.[13] Additional clinical features such as anal, renal, cardiac, ear and foot malformations, hearing loss, postnatal growth retardation, and facial asymmetry have been documented.

Sall1-null mutant mice die perinatally because of severe kidney dysgenesis or agenesis,[14] whereas *Sall2*-deficient mice were reported to show no apparent phenotype.[15] Homozygous *Sall4* knockout mice die shortly after implantation, and *Sall4* haploinsufficiency results in anorectal and heart anomalies as well as exencephaly.[16] Mice lacking both *Sall1* and *Sall2* show kidney phenotypes comparable to those of *Sall1* single knockout mice, suggesting that both genes do not genetically interact *in vivo*. In contrast, *Sall1/4* double heterozygotes exhibit uni- or bilateral renal agenesis, exencephaly, anorectal malformations, and ventricular septum defects with increased incidence in comparison to *Sall4* heterozygotes. This argues for a redundancy in the function of these two *Sall* genes.

Supported by the Deutsche Forschungsgemeinschaft (grants Ko1850/3-2 and Ko1850/6-2 to J. K. and Graduiertenkolleg Molekulare Genetik der Entwicklung to J. K.).

J.B. and A.B. contributed equally to this study.

Accepted for publication July 18, 2008.

Address reprint requests to Prof. Dr. Jürgen Kohlhase, Center for Human Genetics Freiburg, Heinrich-von-Stephan-Str. 5, D-79100 Freiburg, Germany. E-mail: jkohlhase@humangenetik-freiburg.de.

The SALL proteins were shown to be important factors in complex regulatory networks in early and late vertebrate embryogenesis. Murine SALL4 is an essential transcription factor for the early development of inner cell mass-derived cell lineages and is required for the maintenance of embryonic stem cell pluripotency.[17,18] At later stages, SALL4 controls *Fgf10* expression in the limbs and *Gja5* expression in the heart.[19] In zebrafish, *fgf10* expression is indirectly activated by *sall1a* and *sall4* via activation of *fgfr24*.[20] *XsalF* from *Xenopus* determines the position of forebrain and midbrain[21] and *Xsal3*, *csal3*, and *sall1*a are essential for nephrogenesis.[22–24]

Cranial neurulation begins during gastrulation, when the neuroepithelium is induced to differentiate from the dorsal midline ectoderm to form the neural plate. Subsequently, the neural folds form at the edges of the neural plate, elevate from a semihorizontal to a vertical position, and shift from convex to concave in a complex process that involves midline neuroepithelial bending and expansion of the underlying cranial mesenchyme. Later on, the tips of the neural folds converge along the dorsal midline and fuse to form the neural tube.[25–28] Neural tube defects (NTDs) are a group of heterogeneous and complex congenital anomalies of the central nervous system. Most of the mouse NTD mutants reflect a failure in neural fold elevation, and as a consequence, they present as exencephaly, spina bifida, or rachischisis at later stages. In mice, more than 150 mutations have been reported that cause NTDs, but no clinical or experimental study has provided unequivocal evidence for a definitive role for any of these genes in the causation of NTDs in humans. In addition, considerable variation is seen in the pattern of morphogenesis between inbred mouse strains. This indicates that neurogenesis is a complex process with a complex genetic network.

We have generated *Sall2*-null mutant mice, and in contrast to previous reports, we present evidence that *Sall2* has a role in neurogenesis. The incidence of NTDs in *Sall2*$^{-/-}$ embryos is drastically increased in *Sall2/4* compound mutants. In addition, compound *Sall1/4* mutants also display NTDs similar to *Sall2/4* mutants, suggesting an *in vivo* redundant role for the *Sall* genes during murine neurulation.

Materials and Methods

Generation of Sall2$^{-/-}$ *Mice*

The targeting vector was generated by incorporating the 5′ *Bgl*II/*Bgl*II fragment (4.3 kb) and the 3′ *Bgl*II/*Bam*HI (3.0 kb) fragment into the pTKneo vector (kindly provided by Nils Brose, MPI für Experimentelle Medizin, Göttingen, Germany). The 5′ fragment was subcloned into pBluescript (Stratagene, La Jolla, CA) and subsequently cloned into a *Sal*I-*Cla*I site 5′ of the Neo^r gene. The 3′ fragment was excised from a pBluescript subclone and inserted into a *Bgl*II-*Bam*HI site 3′ of the Neo^r gene. RI cells were electroporated, selected, and clones resistant to G418 were isolated and screened by Southern blot. The DNA isolated from the duplicate plate was digested with *Eco*RI, electrophoresed, transferred on nitrocellulose membrane (Amersham, Little Chalfont, UK), and hybridized to radioactive probes to confirm the correct homologous recombination. Nine of thirty-six clones were correctly targeted. Clones were then injected into 129SV/J blastocysts. Resulting chimeric animals were bred with C57BL/6 or 129SV/J females. Mutant animals studied were of F2 and later generations. Mice were genotyped by using genomic polymerase chain reaction (PCR). For genotyping we used the primer mix: SAF1: 5′-GGCTCACAACCATCCGTAACA-3′; ExR1 5′-ACACCTGCTCACCTCCATCG-3′; NeoR1 5′-GCGCGAATTCGATGATCCTGAACGGC-3′. The size of the amplicon is 400 bp for the wild-type allele and 620 bp for the *Sall2* mutant allele.

Sall2$^{+/-}$ mice on a 129SV/J-DBA/2, 129SV/J-NZW, and 129SV/J-CD1 background were generated by crossing *Sall2*$^{-/-}$ mice on a 129SV/J background to mice on the inbred DBA/2 and NZW and the outbred CD1 background, respectively. *Sall2*$^{-/-}$ embryos from F1 intercrosses were analyzed at E12.5 to E14.5. Inbred NZW mice were obtained from The Jackson Laboratory (Bar Harbor, MA), and inbred DBA/2 and outbred CD1 mice were obtained from Charles River (Lyon, France).

Generation of Sall4$^{+/gt}$ *Mice*

Clone W097E01 (embryonic stem cells 129 × 1/SvJ2) carrying an insertion of the gene trap vector pT1βgeo in intron 1 of the *Sall4* gene (*Sall4*$^{GT(pT1Betageo)1Flo}$, hereafter termed *Sall4*^{gt}) was identified within the German Gene Trap Consortium (GGTC; *www.genetrap.de*).[29] Mutant mice were generated after injection into C57BL/6 blastocyst and resulting chimeras were bred to C57BL/6J females. Mice were genotyped using the primer mix: S4F 5′-TGGGGATTCCGGACTTGCTTC-3′; S4R 5′-TTTAAAAGCGGCGCCACTAGAG-3′; pGEOR6 5′-GAGATGGATTGGCAGATGTAGC-3′. The size of the amplicon is 284 bp for the wild-type allele and 234 bp for the *Sall4*^{gt} mutant allele.

Generation of Sall1$^{+/-}$ *Mice*

The targeting vector was made by insertion of a 5′ 6.2-kb *Xho*I/*Cla*I fragment and a 3′ 1.1-kb *Xba*I fragment into the pTKneo vector. The construct was linearized with *Not*I and transfected into R1 embryonic stem cells. Clones resistant to G418 were isolated, screened, and analyzed as described above to confirm homologous recombination. Twenty-seven of forty-three clones were positive. Clones were then injected into 129SV/J blastocysts. Resulting chimeric animals were bred with C57BL/6 females. Mutant animals studied were of F2 and later generations. Mice were genotyped by using genomic PCR. For genotyping of the wild-type allele, we used the primers Ex2 F164 5′-TGATTACACGACATTTCCTACTG-3′ and SA R164 5′-GACGACTCAAGTAAA AAGCACAA-3′ (fragment size 400 bp). For the recombinant allele, PCR was performed with primers Neo F264 5′-GGCTGACCGCTTCCTCGTG-3′ and SA R164 (fragment size 750 bp).

Histological Analysis

Embryos were collected in phosphate-buffered saline (PBS), fixed in Serra (ethanol:37% formaldehyde:acetic

acid, 6:3:1), embedded in paraffin, and sectioned to 7 μm. Sections were stained with hematoxylin and eosin (H&E). For cell proliferation, sections were stained with rabbit anti-phospho-histone 3 (H3P) antibody (catalog no. 06-570, Upstate, Chicago, IL). Detection of apoptotic cells in paraffin sections was performed using a rabbit anti-caspase 3-active antibody (catalog no. AF-835; R&D Systems, Minneapolis, MN). The ABC kit (Vector Laboratories, Burlingame, CA) was used following the manufacturer's protocol. In every section, the number of stained cells was scored and the surface area of neuroepithelium was determined using the AxioVs40 V 4.4.0.0 software (Zeiss, Jena, Germany). Images were captured by a Zeiss Axiocam MRc5 charge-coupled device camera.

In Situ *Hybridization Analysis*

Whole mount *in situ* hybridization was performed following a standard procedure,[30] with digoxigenin-labeled antisense riboprobes for *Sall2*, *Sall4*,[31] *Fgf8*,[32] and *Msx1*.[33] For expression analysis of *Sall2* a 1082-bp *Sall2* BamHI fragment of exon 2 (Figure 1A) containing sequences coding for the third double zinc finger and 3′-UTR was subcloned into pBluescriptKS (Stratagene).

Intracellular Co-Localization Analysis

For co-localization assays, COS-7 and HEK293 cells were grown on coverslips (5×10^4 cells) and transiently transfected with expression plasmids using Lipofectamine (Invitrogen, Carlsbad, CA). After washing with PBS, the cells were treated with methanol for fixation (10 minutes), washed twice with PBS, and equilibrated in IF buffer [10 mmol/L Tris, pH 7.5, 100 mmol/L NaCl, 0,05% (v/v) Tween20, 1% (w/v) bovine serum albumin] for 30 minutes. Cells were incubated with primary antibodies (anti-FLAG; Sigma-Aldrich, St. Louis, MO; and anti-HA; BD Biosciences, Heidelberg, Germany), washed with PBS, incubated with secondary biotinylated antibodies (Vector Laboratories), and signals were detected using the fluorescent avidin kit (Vector Laboratories). Nuclear counterstaining was accomplished by 4,6-diamidino-2-phenylindole staining showing the location of the nuclei for orientation. Finally, coverslips were mounted on glass slides using Slowfade Gold (Invitrogen) and fluorescence signals were visualized by confocal laser-scanning microscopy.

Quantitative Real-Time Reverse Transcriptase (RT)-PCR

For quantitative real-time RT-PCR (qRT-PCR) total RNA was isolated from E8.5 stage embryos and cDNA was prepared by reverse transcription using oligo(dT) primers. The relative expression of the *Sall4* exon 1-2 transcript was analyzed using the primers E1RTF1 (5′-GAAGCCCCAGCACATCAAC-3′) and E2RTR2 (5′-CTGAGGCTTCATCGCAGTT-3′). The exon 1a-2 transcript was amplified with the primer pair E1aRTF1 (5′-CGGACTGCGACACACACC-3′) and E2RTR2. The qRT-PCR was performed using the ABI Prism Real-Time Detection System 7900 (Applied Biosystems, Darmstadt, Germany). For the quantification of RT-PCR products, we used the SYBR Green assay system (Qiagen, Hilden, Germany) according to the manufacturer's instructions. In brief, the RT-PCR reactions were prepared by adding 5 μl of 2× SYBR Green mix, 2.5 μl of primer mix (forward and reverse, 1 pmol/μl), and 2.5 μl of cDNA template. The RT-PCR amplification condition was the following: 94°C 30 seconds, 63°C 30 seconds, 72°C 30 seconds for 45 cycles. Data analysis was done by SDS 2.1 software (Applied Biosystems) using standard curve method and Microsoft Office Excel (Microsoft, Redmond, WA). To verify the specificity and efficiency of real-time analysis, the PCR products were analyzed by monitoring their dissociation curves. The expression levels of investigated transcripts were normalized to β-actin mRNA expression to compensate for difference in sample amounts. The primer sequences used for amplification of the β-actin transcript were actinF (5′-CTTTGCAGCTCCTTCGTTGC-3′) and actinR (5′-ACGATGGAGGGGAATACAGC-3′).

Northern Blot

For expression analysis of *Sall2* a 1082-bp *Sall2 Bam*HI fragment[34] containing sequences coding for the third double zinc finger and 3′ UTR (exon 2) was subcloned into pBluescriptKS (Stratagene). A ^{32}P-labeled probe of this subclone was generated by use of Rediprime II labeling system (Amersham Biosciences) and hybridized to Northern blots containing RNA of adult murine kidney tissue. RNA extraction, Northern blotting, and hybridization were performed as described.[35]

Results

Sall2$^{-/-}$ *Embryos Show NTDs*

We have generated *Sall2*$^{-/-}$ mice by deletion of exons 1a and 2 via homologous recombination, resulting in a loss of all regions encoding zinc finger domains and loss of the complete coding region for the exon 1a-exon 2 transcript (Figure 1, A–C). *Sall2*$^{+/-}$ mice developed normally and had no phenotypic abnormalities. When intercrossed to generate homozygous *Sall2*$^{-/-}$ mutants, again no phenotypic abnormalities were observed on a mixed 129SV/J-C57BL/6 background (105 *Sall2*$^{-/-}$ embryos analyzed). However, when we analyzed *Sall2*$^{-/-}$ mice on a 129SV/J background, the litter size was constantly below the strain-specific average. We therefore decided to analyze the phenotypic appearance of the embryos and noted a significant perinatal lethality (data not shown). We observed abnormalities during neural tube development at E9.5 (Figure 1E) and exencephaly at E11.5 in some *Sall2*$^{-/-}$ embryos (Figure 1G). To quantify the frequency of the phenotype, we collected 208 *Sall2*$^{-/-}$ embryos at E14.5, and 24 (11.5%) embryos displayed exencephaly (Figure 1I). While this work was in progress, a *Sall2*$^{-/-}$ mouse was described. Because these mutants developed to term without pathological findings, a dis-

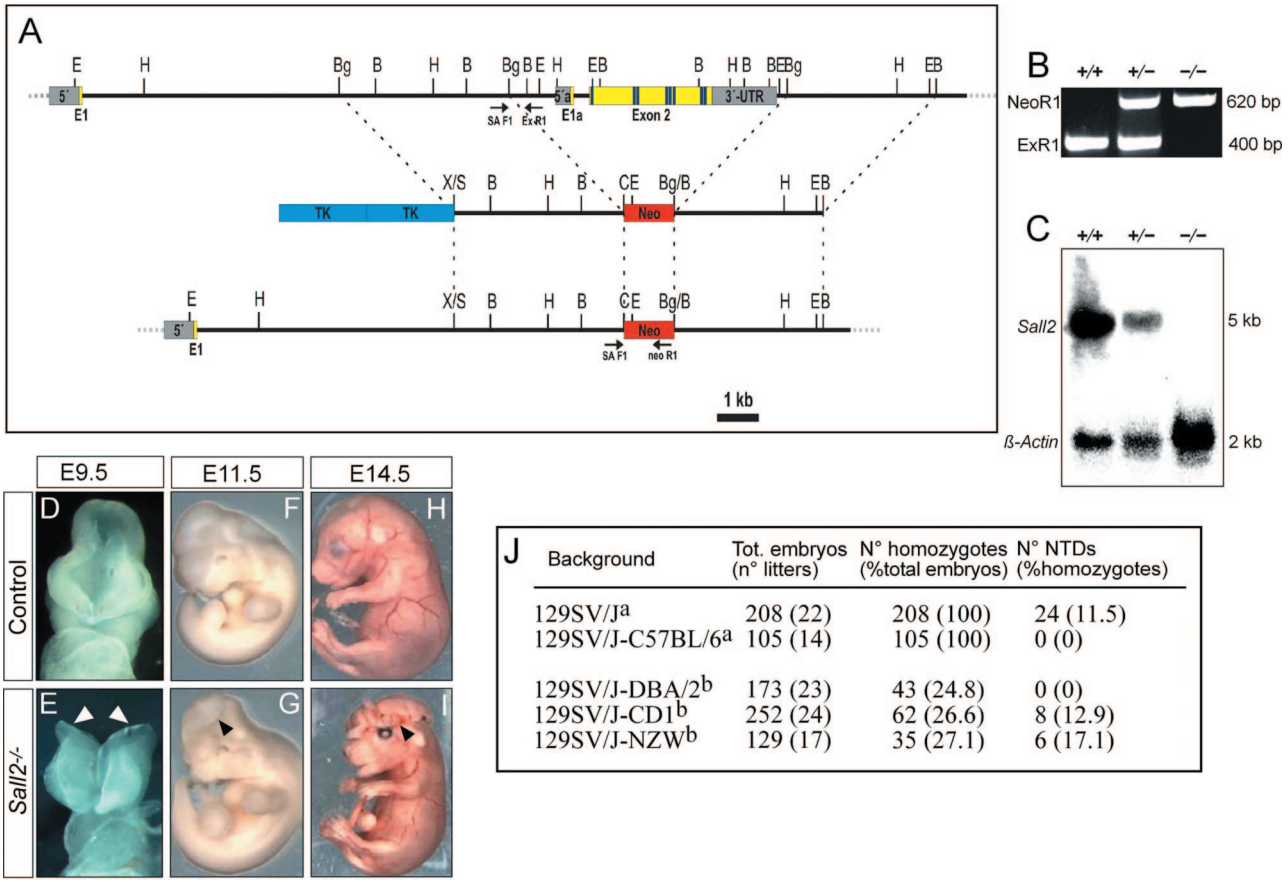

J

Background	Tot. embryos (n° litters)	N° homozygotes (%total embryos)	N° NTDs (%homozygotes)
129SV/J[a]	208 (22)	208 (100)	24 (11.5)
129SV/J-C57BL/6[a]	105 (14)	105 (100)	0 (0)
129SV/J-DBA/2[b]	173 (23)	43 (24.8)	0 (0)
129SV/J-CD1[b]	252 (24)	62 (26.6)	8 (12.9)
129SV/J-NZW[b]	129 (17)	35 (27.1)	6 (17.1)

Figure 1. Generation and analysis of *Sall2*$^{-/-}$ mice. **A:** Strategy for inactivation of the *Sall2* gene. Exons 1a and 2 were replaced by the neomycin cassette of the pTKneo vector resulting in a recombinant allele. Exons including zinc finger domains (blue stripes), sequencing primers (**arrows**), neomycin cassette (Neo), and thymidine kinase (Tk) are depicted B: BamHl, Bg: Bglll, C: Clal, E: EcoRl, H: Hindlll, S: Sall, X: Xbal. **B:** PCR to identify the *Sall2* wild-type allele (+) and the *Sall2* mutant allele (−). The strategy is indicated in **A**. We used a primer mix with the forward primer SAF1 and the reverse primers ExR1 (for wild-type allele) and NeoR1 (for *Sall2* mutant allele). **C:** Northern-blot analysis of *Sall2*-deficient mice. Each lane contains 20 μg of total RNA prepared from kidneys of wild-type mice (+/+), as well as of heterozygous (+/−) and homozygous (−/−) *Sall2* knockout mice. The *Sall2* probe detects a 5-kb transcript. **D–I:** Gross morphology of *Sall2*$^{-/-}$ embryos at different stages. **D** and **E:** At E9.5, the neural tube is already closed in control embryos (**D**), whereas in some *Sall2*$^{-/-}$ embryos the neural folds remain unfused (**E**, **arrowheads**). **F–I:** At E11.5 and at E14.5 some *Sall2*$^{-/-}$ embryos show excencephaly (**G** and **I**, **arrowheads**). **J:** Incidence of NTDs of *Sall2*$^{-/-}$ embryos on different genetic backgrounds. [a]For the 129SVJ and 129SVJ-C57BL/6 backgrounds, embryos analyzed were from homozygous *Sall2* mutant intercrosses from F3 and later generations; [b]for the other three backgrounds, embryos analyzed were from heterozygous *Sall2* mutant F1 intercrosses.

pensable role for *Sall2* in murine embryogenesis has been postulated.[15] In contrast, our results indicate that *Sall2* is required for normal embryonic neural tube development, depending on the genetic background. To confirm this, we generated *Sall2*$^{-/-}$ mice on three new mixed backgrounds: 129SV/J-DBA/2, 129SV/J-CD1, and 129SV/J-NZW. We found NTDs in homozygous *Sall2* mutants on the 129SV/J-CD1 and the 129SV/J-NZW backgrounds at a frequency of 12.9% and 17.1%, respectively, but not on the 129SV/J-DBA/2 background (Figure 1J). This result confirms that *Sall2* plays a role during neurulation. It also shows that the frequency of NTDs displayed by *Sall2*$^{-/-}$ embryos varies depending on the genetic background, indicating that the different genetic constitutions of the various mouse backgrounds modulates the effect of the loss of *Sall2*.

Early Expression of Sall2 *in the Cranial Region*

Previous studies have revealed *Sall2* expression in the metanephros and the spinal cord at E11.5. At later stages, the expression was localized to the kidney and the brain.[15] Because we observed NTDs in *Sall2*$^{-/-}$ embryos already at E9.5, we decided to study *Sall2* expression at early developmental stages. *In situ* hybridization for *Sall2* revealed expression at E7.5 in the neural ectoderm, the mesoderm, and a broad anterior region of the head (Figure 2A). The same expression pattern was observed at E8.5 (Figure 2B). Later, the expression became restricted to distinct structures: strong signals were seen in the forebrain, midbrain, hindbrain, and the mesonephros at E9.5 (Figure 2, C–E) and at E10.5 (Figure 2, F–H). Analysis of the sections indicated that *Sall2* is expressed dorsally in the neuroepithelium all along the body axis (Figure 2, D and E). In addition, *Sall2* expression could be detected in the otic vesicle at E9.5 (Figure 2, C–E), in the lens placode at E10.5, and in the optic cup at E11.5 (Figure 2, H and J). Starting at E11.5, *Sall2* expression in the neural tube decreased but was maintained in the telencephalon and the third ventricle until E12.5 (Figure 2, I, K, and L). This pattern of expression is consistent with a role of *Sall2* in neurulation.

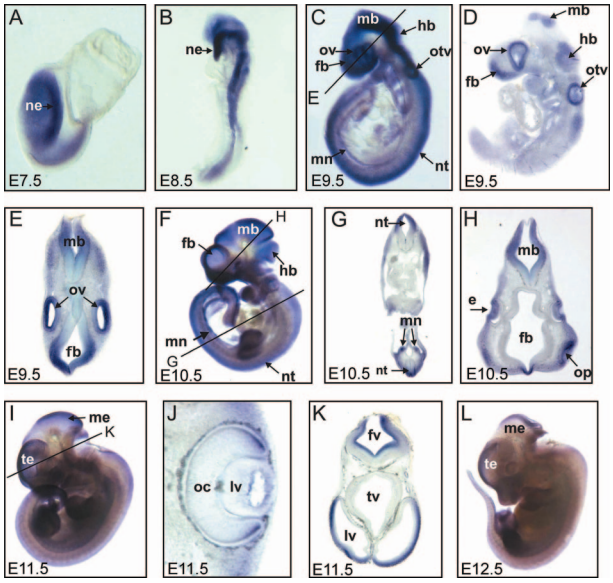

Figure 2. *Sall2* expression during murine embryogenesis. **A–C**, **F**, **I**, and **L:** Whole mount *in situ* hybridization for *Sall2*. **D**, **E**, **G**, **H**, **J**, and **K:** Vibratome sections of the stained embryos. e, eye; fb, forebrain; fv, fourth ventricle; hb, hindbrain; lv, lateral ventricle; mb, midbrain; me, mesencephalon; mn, mesonephros; ne, neuroectoderm; nt, neural tube; oc, optic cup; op, olfactory pit; otv, otic vesicle; ov, optic vesicle; te, telencephalon; tv, third ventricle. For the description of the results see the text.

Redundancy between Sall2 *and* Sall4 *in Neural Tube Development*

The low penetrance of the cranial abnormalities in the *Sall2*$^{-/-}$ embryos might be explained by the compensation by other factors. *Sall4*, a closely related gene, was previously shown to display a similar expression pattern during embryogenesis,[31] and we confirmed by *in situ* hybridization that both genes were simultaneously expressed in the developing neuroectoderm of the cranial region at E8.5 (Figure 3, A and B). To screen for a possible redundant role during neural tube development, we decided to generate compound *Sall2/4* mutant mice.

Heterozygous *Sall4* gene trap mutant mice, *Sall4*$^{+/gt}$, generated as described in the Materials and Methods, did not reveal any phenotypic abnormalities. In contrast, *Sall4*$^{gt/gt}$ homozygous embryos displayed a phenotype similar to *Sall4*-deficient knockout mice,[16] but they died at approximately E7.5, 1 day later than reported for homozygous knockouts (unpublished observations). By database searches we identified an EST clone (BY729264) comprising an alternative first exon upstream of exon 2 that contained a different translation initiation site. Comparison of the EST sequence to the *Sall4* genomic region identified the localization of the alternative exon closely downstream of the genetrap integration site. The newly identified exon was named exon 1a (Figure 3C). To determine the impact of the integration of the gene trap vector we performed quantitative RT-PCR at E7.5. Our analysis revealed that in *Sall4*^{gt} homozygous mutants the mRNA expression initiated from exon 1 was completely abolished whereas the expression initiated from exon 1a was reduced to 45% when compared to wild-type embryos (Figure 3D). Therefore, the genetrap integration resulted in a hypomorphic *Sall4* mutant allele. Analysis of the cross between *Sall2*$^{+/-}$*Sall4*$^{+/gt}$ mice and *Sall2*$^{-/-}$ mice revealed that *Sall2*$^{-/-}$*Sall4*$^{+/gt}$ developed NTDs with a full penetrance of the phenotype (24 of 24), whereas the phenotype was only partially penetrant in *Sall2/4* compound heterozygous mutant embryos (4 of 23). We found no NTDs in the other genetic combinations (Figure 3I).

To determine when phenotypic differences between *Sall2*$^{+/-}$*Sall4*$^{+/gt}$ and control embryos can first be detected, we examined H&E-stained sections of the cranial region between E8.0 to E8.5 (9 to 13 somite stage). At the 9-somite stage, the neural folds are already prominent in the cephalic region of both control and mutant embryos, lying in a semihorizontal position (Figure 3, J–M). At the 11-somite stage, the neural folds in the cephalic region are elevating and start to become parallel in control embryos (Figure 3N). This bending is also visible in the mutant neural folds, but to a much lesser extent, and the distance between the neural tips is always increased (Figure 3O). In a more rostral location, the development of an optic vesicle is visible in both control and mutant embryos (Figure 3, P and Q; arrow), but the distance between the neural tips remains increased in mutant embryos (Figure 3Q). At the 13-somite stage, in control embryos, the neural folds in the cephalic region are lying parallel, and the neural tips are close to fusing (Figure 3R). In the mutant embryos, the degree of bending of the neural folds is similar to the 11-somite stage, and the neural tips are very far apart (Figure 3S). In a more rostral location, the edges of the neural tube are parallel and very close to each other in control embryos (Figure 3T), whereas they are very separated in the mutant embryos (Figure 3U). At E9.5, the neural tube is already fused in control embryos (Figure 3, V and X), whereas the neural folds remain unfused in the mutants (Figure 3, W and Y). Altogether, these results show that *Sall2*$^{-/-}$*Sall4*$^{+/gt}$ embryos have a failure in neural fold elevation and fusion, which finally leads to the excencephally seen at later stages. They also indicate that *Sall2* and *Sall4* have a redundant function in neural tube closure.

Increased Apoptosis in Sall2$^{-/-}$Sall4$^{+/gt}$ *Embryos*

To test whether a complete gene misregulation may be responsible for the phenotype observed in *Sall2*$^{-/-}$*Sall4*$^{+/gt}$ embryos, we analyzed by *in situ* hybridization the expression of *Fgf8*, a marker for the neuroepithelium of the frontonasal region, the midbrain-hindbrain boundary, and the branchial arch,[32] and *Msx1,* that is expressed in the forebrain and the midbrain.[33] No difference in expression was seen for these two markers between *Sall2*$^{-/-}$*Sall4*$^{+/gt}$ and wild-type embryos (Figure 4, A–D). Thus, a significant misregulation of these two marker genes seems not to be the origin of the neural tube closure defects seen in the *Sall2*$^{-/-}$*Sall4*$^{+/gt}$ mutant embryos.

To test whether the neuroepithelium of *Sall2*$^{-/-}$*Sall4*$^{+/gt}$ mutants may reveal any difference in cell proliferation or cell death we performed immunohistochemistry for the mitosis marker H3P and for the apoptotic marker caspase

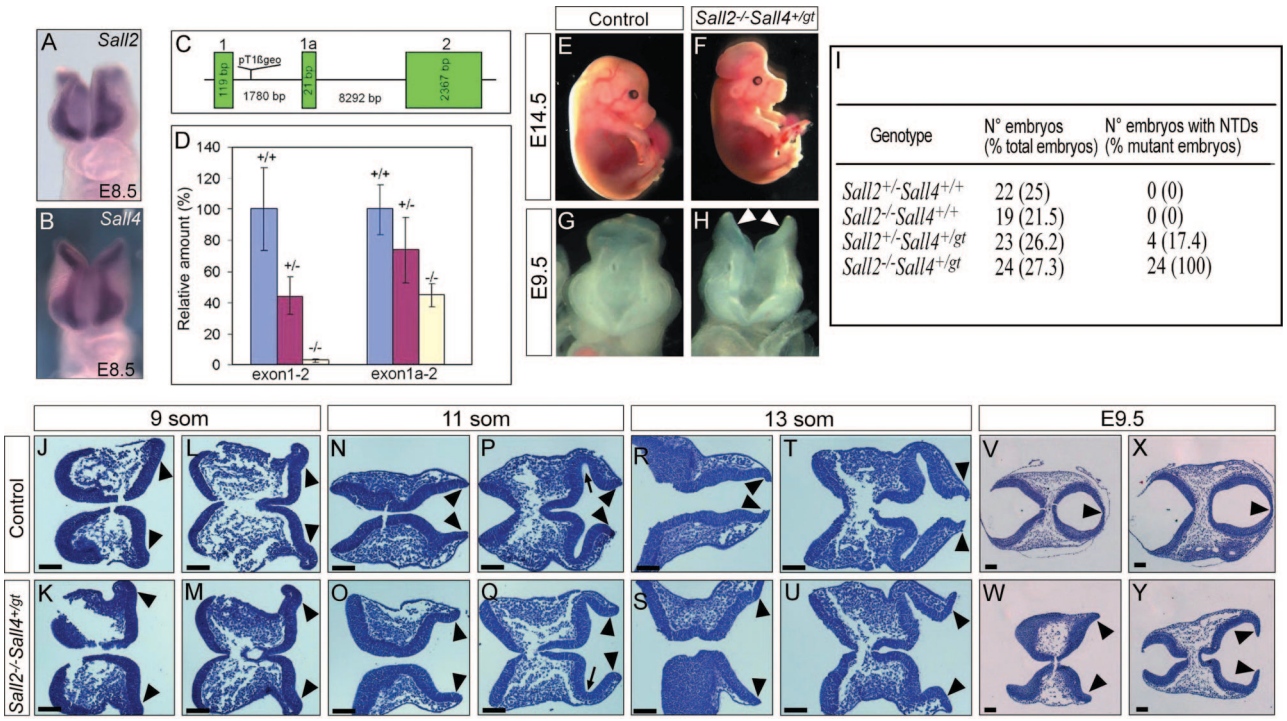

Figure 3. Analysis of *Sall2/4* compound mutants. **A** and **B:** *In situ* hybridization for *Sall2* (**A**) and for *Sall4* (**B**) on mouse embryos revealed that both genes have a similar pattern of expression in the cranial neuroepithelium at E8.5. **C:** Schematic representation of the integration of the pT1βgeo gene trap vector in the *Sall4* locus. Only the first three exons are shown. Integration occurred in intron 1, between exon 1 and the newly identified alternative exon 1a. **D:** Quantitative RT-PCR of E7.5 wild-type (+/+) and heterozygous (+/−) and homozygous (−/−) $Sall4^{gt}$ embryos for the *Sall4* locus. Primers were designed to include either exon 1 and exon 2 (exon1–2) or exon 1a and exon 2 (exon 1a-2). Note that in $Sall4^{gt/gt}$ embryos, exon1–2 transcripts are abolished whereas 45% of exon 1a-2 transcripts are still present when compared to wild-type embryos. **E–H:** $Sall2^{-/-}Sall4^{+/gt}$ embryos at E14.5 showed exencephaly (**F**). At E9.5, the forebrain and midbrain neural folds of mutant embryos did not fuse (**H**, **arrowheads**). **I:** Incidence of NTDs in the four mutant genotypes resulting from the cross between $Sall2^{+/-}Sall4^{+/gt}$ mice and $Sall2^{-/-}$ mice. **J–Y:** Transverse serial sections of controls (**J**, **L**, **N**, **P**, **R**, **T**, **V**, **X**) and $Sall2^{-/-}Sall4^{+/gt}$ embryos (**K**, **M**, **O**, **Q**, **S**, **U**, **W**, **Y**) stained with H&E demonstrated a failure in elevation and central fusion of the neural folds in the mutants. **Arrowheads** point to the tips of the neural folds, and **arrows** (**P**, **Q**) point to the optic vesicle. For a detailed explanation see the text. Scale bars = 100 μm.

3 at the 9- to 13-somite stage. We found no difference in cell proliferation between control and mutant embryos (Figure 4E, top). In contrast, we found an increased number of apoptotic cells (Figure 4E, bottom). Analysis of the neuroepithelium of control embryos stained for caspase 3 revealed some positive cells, in particular close to the bending of the neural tube (Figure 4, F, H, and J). In the equivalent regions in the mutants the number of positive cells was markedly increased (Figure 4, G, I, and K).

Sall1 *and* Sall4 *Act Redundantly during Murine Neurulation*

The murine *Sall1* gene is closely related to *Sall2* and *Sall4* and is also expressed in the neural tube. In compound *Sall1/2*-null mutants no neural tube abnormalities have been described.[15] To screen for a possible redundant role between *Sall1* and *Sall4* in murine neurulation, we crossed $Sall1^{+/-}$ mice to mice harboring the hypomorphic $Sall4^{gt}$ allele. For this purpose we generated $Sall1^{+/-}$ mice by homologous recombination resulting in a deletion of exons 2 and 3 including all zinc finger domains. Heterozygous *Sall1* mutant mice were phenotypically normal and fertile, whereas homozygous *Sall1* mutants died perinatally as a result of a bilateral kidney agenesis, as previously described.[14]

By crossing $Sall1^{+/-}$ and $Sall4^{+/gt}$ mice we obtained 4 $Sall1^{+/-}Sall4^{+/gt}$ mutants of 79 offspring. While this work was in progress, a *Sall1/4* compound heterozygous mutant was described. Interestingly, 45% of these $Sall1^{+/-}Sall4^{+/-}$ mutants showed NTDs, but none of them survived after birth.[16] We therefore speculate that the remaining expression of our $Sall4^{gt}$ hypomorphic allele (see above) may account for the incomplete penetrance and therefore may rescue a small number of embryos from early lethality.

Analysis of the embryos from the cross between $Sall1^{+/-}Sall4^{+/gt}$ mice and $Sall1^{+/-}$ mice revealed that $Sall1^{-/-}Sall4^{+/gt}$ embryos presented with general growth retardation at E10.5 and died at approximately E11.5, probably because of cardiac failure (data not shown); they developed NTDs with a full penetrance of the phenotype (eight of eight) (Figure 5, E and F). In contrast the phenotype was partially penetrant in $Sall1^{+/-}Sall4^{+/gt}$ compound heterozygous mutant embryos (9 of 20) (Figure 5, B, D, and F). We found no NTDs in the other genetic combinations (Figure 5F). In conclusion, our data suggest that the higher the dosage of *Sall4* on a $Sall1^{+/-}$ background, or the higher the dosage of *Sall1* on a $Sall4^{+/gt}$ background, the less severe is the penetrance of the resulting cranial phenotype. This supports the idea of functional redundancy of both genes during murine neurulation.

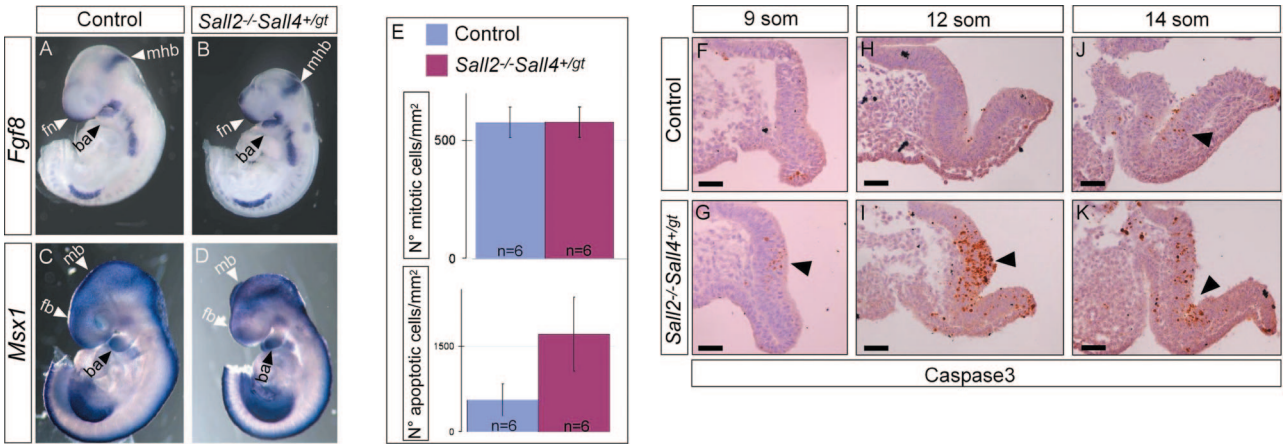

Figure 4. Increased apoptosis in *Sall2*$^{-/-}$*Sall4*$^{+/gt}$ neural folds. **A–D:** *In situ* hybridization for *Fgf8* and *Msx1* at E9.5 revealed no difference in the pattern of expression of both genes between control (**A**, **C**) and *Sall2*$^{-/-}$*Sall4*$^{+/gt}$ embryos (**B**, **D**). **E:** Analysis of cell proliferation and apoptosis of control and *Sall2*$^{-/-}$*Sall4*$^{+/gt}$ mutant embryos at 9 to 13 somite stages. For cell proliferation no statistical difference was found between controls and *Sall2*$^{-/-}$*Sall4*$^{+/gt}$ embryos ($n = 6$; unpaired *t*-test, $P = 0.9554$) (**E**, **top**). In contrast, a statistically significant difference was seen in the number of apoptotic cells between control and *Sall2*$^{-/-}$*Sall4*$^{+/gt}$ embryos ($n = 6$; unpaired *t*-test, $P = 0.0026$) (**E**, **bottom**). **F**, **H**, and **J:** Analysis of the neuroepithelium of control embryos stained for caspase 3 revealed some positive cells, in particular close to the bending of the neural tube (**arrowhead** in **J**). **G**, **I,** and **K:** In the equivalent regions of *Sall2*$^{-/-}$*Sall4*$^{+/gt}$ embryos the number of positive cells was markedly increased. **Arrowheads** point to the apoptotic cells. ba, branchial arch; fb, forebrain; mhb, midbrain-hindbrain boundary; fn, frontonasal region; mb, midbrain. Scale bars = 50 μm.

It has previously been shown that SALL1 and SALL4 are located in distinct nuclear dots representing heterochromatic structures.[36,37] We therefore investigated whether SALL1, SALL2, and SALL4 co-localize in the nucleus. By triple-transfecting COS-7 cells with fusion proteins SALL1-GFP, SALL2-Flu, and SALL4-FLAG we found that SALL2 and SALL4 preferentially co-localize at the nuclear margins, whereas SALL1 is more centrally located. However, all proteins co-localize in dot-like structures in the nucleus, favoring the idea that they may operate as redundant transcription factors (Figure 5, G–J).

Discussion

Previous data suggested a dispensable role for *Sall2* in embryogenesis because no human disease is associated with mutations in the *SALL2* gene and because *Sall2*$^{-/-}$ mice do not present any phenotypic abnormalities.[15] In contrast, here we present evidence that *Sall2* may have a role in neurulation as we found NTDs in *Sall2*-deficient mice. Our *Sall2*-null mutant embryos presented this phenotypic abnormality only on a 129SV/J background, but not on a mixed 129SV/J-C57BL/6 background, the background of the *Sall2* mutants described

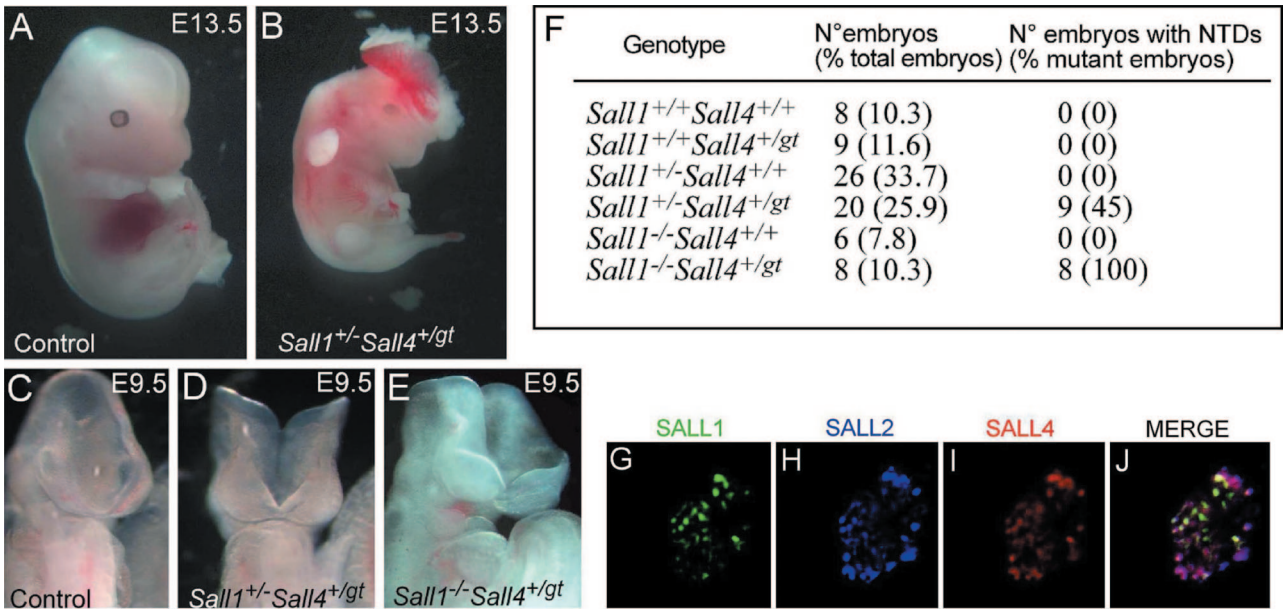

Figure 5. Analysis of *Sall1/4* compound mutants. **A** and **B:** Gross morphology at E13.5 of a control embryo (**A**) and a *Sall1/4* double heterozygous mutant embryo presenting exencephaly (**B**). **C–E:** At E9.5, some of the *Sall1/4* double heterozygous embryos displayed defects in neural tube closure (**D**). All *Sall1*$^{-/-}$*Sall4*$^{+/gt}$ embryos obtained showed a severe phenotype at E9.5 (**E**). **F:** Incidence of NTDs in the different genotypes resulting from the cross between *Sall1*$^{+/-}$*Sall4*$^{+/gt}$ mice and *Sall1*$^{+/-}$ mice. **G–J:** Intracellular co-localization of SALL1, SALL2, and SALL4. COS-7 cells expressing SALL1-GFP (green), SALL2-Flu (blue), and SALL4-FLAG (red) showed that SALL2 and SALL4 essentially co-localized at the nuclear periphery, whereas SALL1 showed a more homogenous distribution.

by Sato and colleagues.[15] To confirm this phenomenon of strain-specific variations in the penetrance of the phenotype, we studied *Sall2*$^{-/-}$ mice on three other backgrounds, and found that *Sall2*$^{-/-}$ mice also developed NTDs on the mixed backgrounds 129SV/J-CD1 and 129SV/J-NZW, but not on a mixed 129SV/J-DBA/2 background. These data are consistent with the notion that genetic loci controlling neural tube development are polymorphic between the mouse strains. Indeed, strain-specific variations in the penetrance of NTDs displayed by homozygous null mutants have been frequently reported. One of the factors that may affect these strain-specific differences in NTDs is the position of neural tube closure 2, which varies between mouse strains.[38,39] The position of closure 2 is located within the midbrain in the DBA/2 strain, is located more rostrally, at the midbrain-forebrain boundary, in the CD1 strain and is located even more rostrally, in the forebrain, in the NZW strain.[38] A rostral location of closure 2 has been proposed to be a risk factor for cranial NTDs. Accordingly, in *Sp*^{2H} mutants, the frequency of cranial NTDs is reduced after transfer to the DBA/2 background and is increased after transfer to the NZW background.[38] Consistent with these data, we found no NTDs in embryos on the mixed 129SV/J-DBA/2 background, but we did observe NTDs in embryos on the 129SV/J-CD1 and 129SV/J-NZW backgrounds. Our data are thus consistent with the notion that a protective role of caudal closure 2 may account for the differences in the penetrance of NTDs seen in our *Sall2*-deficient mice. As nothing is known up to now where site 2 closure occurs in the 129SV and the C57BL/6 strains, it is not possible to discuss whether or not the absence of NTDs observed in *Sall2*$^{-/-}$ mutant mice on the mixed 129SV/C57BL/6 background may be because of a caudal site 2 closure protective effect. But one must also consider that we analyzed mixed genetics backgrounds, thus, the shift in the position of closure 2 was not as prominent as on a pure genetic background. So, in addition to the position of closure 2, other genetic factors must be involved in the strain-specific differences observed.

The low incidence of NTDs in *Sall2*$^{-/-}$ embryos, the similar structure of the SALL proteins, the overlapping expression patterns of *Sall1*, *Sall2*, and *Sall4* in the cranial region, and the overlapping clinical features of patients with TBS and Okihiro syndrome led us to the hypothesis of a redundant function of the SALL proteins in neurogenesis. We therefore generated *Sall2/4* and *Sall1/4* compound mutants. Morphological analyses of the embryos revealed that the higher the SALL dosage, the less penetrant were the NTDs. In addition, we showed that SALL1, SALL2, and SALL4 co-localize in the nucleus, and previous GST-pulldown studies have demonstrated that the SALL proteins form homo- and heterodimers.[40] These *in vivo* and *in vitro* results indicate an essential and redundant role of the murine *Sall* genes in neurulation.

Histological analysis of our *Sall2/4* compound mutants revealed a failure in the elevation of the neural folds in the forebrain and midbrain. In *Sall2*$^{-/-}$*Sall4*$^{+/gt}$ embryos the neural folds remain in a semihorizontal position and they never elevate and fuse. The exencephaly shown by mutant embryos at later stages is probably a direct consequence of the failure in elevation. Taken together, these results indicate that *Sall2/4* have an essential role in the process of neural fold elevation during neurogenesis.

Neural tube closure is a complex and multistep process that involves lifting, bending, and fusion of the neural folds. Therefore, cell proliferation and cell death must be tightly regulated during this process. We did not find increased cell proliferation in *Sall2*$^{-/-}$*Sall4*$^{+/gt}$ embryos, but we detected an increased number of apoptotic cells. Little is known about the molecular function of *Sall2* and *Sall4*. *Sall2* has been proposed to act in some cell types as a regulator of cell growth and survival,[11] and *Sall4* has been shown to be a regulator of survival and apoptosis in human leukemic cells.[41] It is thus conceivable that both genes may have an anti-apoptotic function also during early neural development. Alternatively, *Sall2/4* may control other unknown function(s) during neurulation, and the increased number of apoptotic cells may simply be a consequence of the failure in neural fold elevation.

NTDs are only rarely seen in TBS and Okihiro syndrome. In TBS, two families are known to us in which some affected members have Arnold-Chiari malformation type 1. In Okihiro syndrome, one patient with a *SALL4* deletion was born with a meningomyelocele (J. Kohlhase, unpublished data). Therefore, NTDs are a rare feature associated with heterozygous *SALL1* or *SALL4* mutations in humans. However, it is conceivable that compound mutations in *SALL1*, *SALL2*, or *SALL4* may result in defective neural tube closure also in humans. But such a severe phenotype would implicate embryonic lethality and hence escape the clinical diagnosis of TBS or Okihiro syndrome. Mutations in *SALL2* have not yet been correlated with a human disease, and this may be because of the compensatory character of the other *SALL* genes. This assumption is strengthened by the fact that *Sall2*$^{+/-}$ mice are phenotypically normal and that *Sall2*$^{-/-}$ embryos exhibit a reduced penetrance of the NTDs (~10%) only in some mouse strains. It is therefore likely that the heterozygous loss of SALL2 can effectively be compensated by the related SALL proteins in human.

Acknowledgments

We thank Monika Schindler, Henning Riedesel, and Stefan Wolf for expert assistance in the generation of knockout mice; Gerd Scherer, Annette Neubüser, and Alexander Craig for critical review of the manuscript; and Pauline Soulas and Jean-Louis Pasquali for the kind gift of NZW mice.

References

1. Jürgens G: Head and tail development of the Drosophila embryo involves spalt, a novel homeotic gene. EMBO J 1988, 7:189–196
2. Kühnlein RP, Frommer G, Friedrich M, Gonzalez-Gaitan M, Weber A, Wagner-Bernholz JF, Gehring W, Jäckle H, Schuh R: spalt encodes an evolutionary conserved zinc finger protein of novel structure which provides homeotic gene function in the head and tail region of the Drosophila embryo. EMBO J 1994, 13:168–179
3. de Celis J, Barrio R, Kafatos F: A gene complex acting downstream of dpp in Drosophila wing morphogenesis. Nature 1996, 381:421–424

4. de Celis JF, Barrio R, Kafatos FC: Regulation of the spalt/spalt-related gene complex and its function during sensory organ development in the Drosophila thorax. Development 1999, 126:2653–2662
5. Kühnlein RP, Schuh R: Dual function of the region specific homeotic gene spalt during Drosophila tracheal system development. Development 1996, 122:2215–2223
6. Nellen D, Burke R, Struhl G, Basler K: Direct and long-range action of a DPP morphogen gradient. Cell 1996, 85:357–368
7. Kohlhase J, Wischermann A, Reichenbach H, Froster U, Engel W: Mutations in the SALL1 putative transcription factor gene cause Townes-Brocks syndrome. Nat Genet 1998, 18:81–83
8. Powell CM, Michaelis RC: Townes-Brocks syndrome. J Med Genet 1999, 36:89–93
9. Surka WS, Kohlhase J, Neunert CE, Schneider DS, Proud VK: Unique family with Townes-Brocks syndrome, SALL1 mutation, and cardiac defects. Am J Med Genet 2001, 102:250–257
10. Li D, Dower K, Ma Y, Tian Y, Benjamin T: A tumor host range selection procedure identifies p150(sal2) as a target of polyoma virus large T antigen. Proc Natl Acad Sci USA 2001, 98:14619–14624
11. Li D, Tian Y, Ma Y, Benjamin T: p150(Sal2) is a p53-independent regulator of p21(WAF1/CIP). Mol Cell Biol 2004, 24:3885–3893
12. Kohlhase J, Hausmann S, Stojmenovic G, Dixkens C, Bink K, Schulz-Schaeffer W, Altmann M, Engel W: SALL3, a new member of the human spalt-like gene family, maps to 18q23. Genomics 1999, 62:216–222
13. Kohlhase J, Chitayat D, Kotzot D, Ceylaner S, Froster U, Fuchs S, Montgomery T, Rösler B: SALL4 mutations in Okihiro syndrome (Duane-radial ray syndrome), acro-renal-ocular syndrome, and related disorders. Hum Mutat 2005, 26:176–183
14. Nishinakamura R, Matsumoto Y, Nakao K, Nakamura K, Sato A, Copeland NG, Gilbert DJ, Jenkins NA, Scully S, Lacey DL, Katsuki M, Asashima M, Yokota T: Murine homolog of SALL1 is essential for ureteric bud invasion in kidney development. Development 2001, 128:3105–3115
15. Sato A, Matsumoto Y, Koide U, Kataoka Y, Yoshida N, Yokota T, Asashima M, Nishinakamura R: Zinc finger protein sall2 is not essential for embryonic and kidney development. Mol Cell Biol 2003, 23:62–69
16. Sakaki-Yumoto M, Kobayashi C, Sato A, Fujimura S, Matsumoto Y, Takasato M, Kodama T, Aburatani H, Asashima M, Yoshida N, Nishinakamura R: The murine homolog of SALL4, a causative gene in Okihiro syndrome, is essential for embryonic stem cell proliferation, and cooperates with Sall1 in anorectal, heart, brain and kidney development. Development 2006, 133:3005–3013
17. Elling U, Klasen C, Eisenberger T, Anlag K, Treier M: Murine inner cell mass-derived lineages depend on Sall4 function. Proc Natl Acad Sci USA 2006, 103:16319–16324
18. Zhang J, Tam WL, Tong GQ, Wu Q, Chan HY, Soh BS, Lou Y, Yang J, Ma Y, Chai L, Ng HH, Lufkin T, Robson P, Lim B: Sall4 modulates embryonic stem cell pluripotency and early embryonic development by the transcriptional regulation of Pou5f1. Nat Cell Biol 2006, 8:1114–1123
19. Koshiba-Takeuchi K, Takeuchi JK, Arruda EP, Kathiriya IS, Mo R, Hui CC, Srivastava D, Bruneau BG: Cooperative and antagonistic interactions between Sall4 and Tbx5 pattern the mouse limb and heart. Nat Genet 2006, 38:175–183
20. Harvey SA, Logan MP: Sall4 acts downstream of tbx5 and is required for pectoral fin outgrowth. Development 2006, 133:1165–1173
21. Onai T, Sasai N, Matsui M, Sasai Y: Xenopus XsalF: anterior neuroectodermal specification by attenuating cellular responsiveness to Wnt signaling. Dev Cell 2004, 7:95–106
22. Camp E, Hope R, Kortschak RD, Cox TC, Lardelli M: Expression of three spalt (sal) gene homologues in zebrafish embryos. Dev Genes Evol 2003, 213:35–43
23. Farrell ER, Tosh G, Church E, Munsterberg AE: Cloning and expression of CSAL2, a new member of the spalt gene family in chick. Mech Dev 2001, 102:227–230
24. Onuma Y, Nishinakamura R, Takahashi S, Yokota T, Asashima M: Molecular cloning of a novel Xenopus spalt gene (Xsal-3). Biochem Biophys Res Commun 1999, 264:151–156
25. Copp AJ: Neurulation in the cranial region—normal and abnormal. J Anat 2005, 207:623–635
26. Harris MJ, Juriloff DM: Mouse mutants with neural tube closure defects and their role in understanding human neural tube defects. Birth Defects Res A Clin Mol Teratol 2007, 79:187–210
27. Juriloff DM, Harris MJ: Mouse models for neural tube closure defects. Hum Mol Genet 2000, 9:993–1000
28. Padmanabhan R: Etiology, pathogenesis and prevention of neural tube defects. Congenit Anom (Kyoto) 2006, 46:55–67
29. Wiles MV, Vauti F, Otte J, Fuchtbauer EM, Ruiz P, Fuchtbauer A, Arnold HH, Lehrach H, Metz T, von Melchner H, Wurst W: Establishment of a gene-trap sequence tag library to generate mutant mice from embryonic stem cells. Nat Genet 2000, 24:13–14
30. Wilkinson DG, Nieto MA: Detection of messenger RNA by in situ hybridization to tissue sections and whole mounts. Methods Enzymol 1993, 225:361–373
31. Kohlhase J, Heinrich M, Liebers M, Froehlich Archangelo L, Reardon W, Kispert A: Cloning and expression analysis of Sall4, the murine homologue of the gene mutated in Okihiro syndrome. Cytogenet Genome Res 2002, 98:274–277
32. Crossley PH, Martin GR: The mouse Fgf8 gene encodes a family of polypeptides and is expressed in regions that direct outgrowth and patterning in the developing embryo. Development 1995, 121: 439–451
33. Catron KM, Wang H, Hu G, Shen MM, Abate-Shen C: Comparison of MSX-1 and MSX-2 suggests a molecular basis for functional redundancy. Mech Dev 1996, 55:185–199
34. Kohlhase J, Altmann M, Archangelo L, Dixkens C, Engel W: Genomic cloning, chromosomal mapping, and expression analysis of Msal-2. Mamm Genome 2000, 11:64–68
35. Buck A, Archangelo L, Dixkens C, Kohlhase J: Molecular cloning, chromosomal localization, and expression of the murine SALL1 ortholog Sall1. Cytogenet Cell Genet 2000, 89:150–153
36. Böhm J, Kaiser FJ, Borozdin W, Depping R, Kohlhase J: Synergistic cooperation of Sall4 and cyclin D1 in transcriptional repression. Biochem Biophys Res Commun 2007, 356:773–779
37. Netzer C, Rieger L, Brero A, Zhang C-D, Hinzke M, Kohlhase J, Bohlander SK: SALL1, the gene mutated in Townes-Brocks syndrome, encodes a transcriptional repressor which interacts with TRF1/ PIN2 and localizes to pericentromeric heterochromatin. Hum Mol Genet 2001, 10:3017–3024
38. Fleming A, Copp AJ: A genetic risk factor for mouse neural tube defects: defining the embryonic basis. Hum Mol Genet 2000, 9:575–581
39. Juriloff DM, Harris MJ, Tom C, MacDonald KB: Normal mouse strains differ in the site of initiation of closure of the cranial neural tube. Teratology 1991, 44:225–233
40. Sweetman D, Smith T, Farrell ER, Chantry A, Münsterberg A: The conserved glutamine rich region of chick csal1 and csal3 mediates protein interactions with other spalt family members. Implications for Townes-Brocks syndrome. J Biol Chem 2003, 278:6560–6566
41. Yang J, Chai L, Gao C, Fowles TC, Alipio Z, Dang H, Xu D, Fink LM, Ward DC, Ma Y: SALL4 is a key regulator of survival and apoptosis in human leukemic cells. Blood 2008, 112:805–813